Relative Reactivity of Biogenic and Chemogenic Uraninite and Biogenic Non-Crystalline U(IV)

José M. Cerrato[1], Matthew N. Ashner[1], Daniel S. Alessi [2], Juan S. Lezama-Pacheco[3†], Rizlan Bernier-Latmani[2], John R. Bargar[3], and Daniel E. Giammar[1]*

[*] Corresponding email address: cerratoj@wustl.edu

Telephone: (001) (314) 935-3457

Fax: (001) (314) 935-5464

[1] Department of Energy, Environmental, and Chemical Engineering, One Brookings Drive, Washington University, Saint Louis, Missouri 63130

[2] Environmental Microbiology Laboratory, École Polytechnique Fédérale de Lausanne, Lausanne, CH 1015, Switzerland

[3] Stanford Synchrotron Radiation Lightsource, SLAC, 2575 Sand Hill Road, Menlo Park, California 94025

[†] Present address: Department of Earth & Earth System Science, Stanford University, Stanford, California 94305, USA

Journal: Environmental Science & Technology

Date: July 25, 2013

10 pages (including cover page)

2 Tables

6 Figures

Content:

Table S1. Composition of Widdel Low Phosphate (WLP) medium used to favor the production of monomeric U(IV) species during microbial U(VI) reduction. WLP is comprised of 1 mL of solutions B, C, and D, added to 1 L of solution A.

A

Component	g L^{-1}
Calcium chloride	0.1
Potassium chloride	0.5
Monopotassium phosphate	0.03
Magnesium chloride	0.5
Sodium chloride	5.0
Ammonium chloride	0.25
Sodium bicarbonate	3.7
PIPES buffer	6.0
Lactic acid	1.8
Yeast Extract	0.5

B

Component	g L^{-1}
Hydrochloric acid	14.75
Ferrous sulfate	2.1
Boric acid	0.03
Manganese chloride	0.1
Cobalt chloride	0.19
Nickel chloride	0.024
Copper chloride	0.002
Zinc sulfate	0.144
Sodium molybdate	0.036

C

Component	g L^{-1}
4-aminobenzoic acid	0.04
D(+)-biotin	0.01
Nicotinic acid	0.1
Calcium D(+) pantothenate	0.05
Pyrodoxine dihydrochloride	0.15

D

Component	g L^{-1}
Sodium hydroxide	0.4
Sodium tungstate	0.008
Selenious acid	0.0025

Table S2. Thermodynamic stability constants (T = 25°C, I = 0) used for MINEQL dissolved U calculations conducted to evaluate the reactions of various ligands with chemogenic uraninite.

Reaction	Log K
U(IV) aqueous species	
$U^{4+} + H_2O = UOH^{3+} + H^+$	-0.54
$U^{4+} + 2\ H_2O = U(OH)_2^{2+} + 2\ H^+$	-1.10
$U^{4+} + 3\ H_2O = U(OH)_3^{+} + 3\ H^+$	-4.70
$U^{4+} + 4\ H_2O = U(OH)_4 + 4\ H^+$	-10.00
$U^{4+} + 2\ CO_3^{2-} + 2\ H_2O = U(OH)_2(CO_3)_2^{2-} + 2\ H^+$	14.40
$U^{4+} + 4\ CO_3^{2-} = U(CO_3)_4^{4-}$	35.12
$U^{4+} + 5\ CO_3^{2-} = U(CO_3)_5^{6-}$	34.00
$U^{4+} + F^- = UF^{3+}$	9.42
$U^{4+} + 2F^- = UF_2^{2+}$	16.56
$U^{4+} + 3F^- = UF_3^{+}$	21.89
$U^{4+} + 4F^- = UF_4$	26.34
$U^{4+} + 5F^- = UF_5^-$	27.73
$U^{4+} + 6F^- = UF_6^{2-}$	29.80
$U^{4+} + edta^{4-} = Uedta(aq)$	-29.50
U(IV) solid species	
$U^{4+} + 2\ H_2O = UO_{2(crystal)} + 4\ H^+$	4.85
$U^{4+} + 2\ H_2O = UO_{2(amorphous)} + 4\ H^+$	-1.50

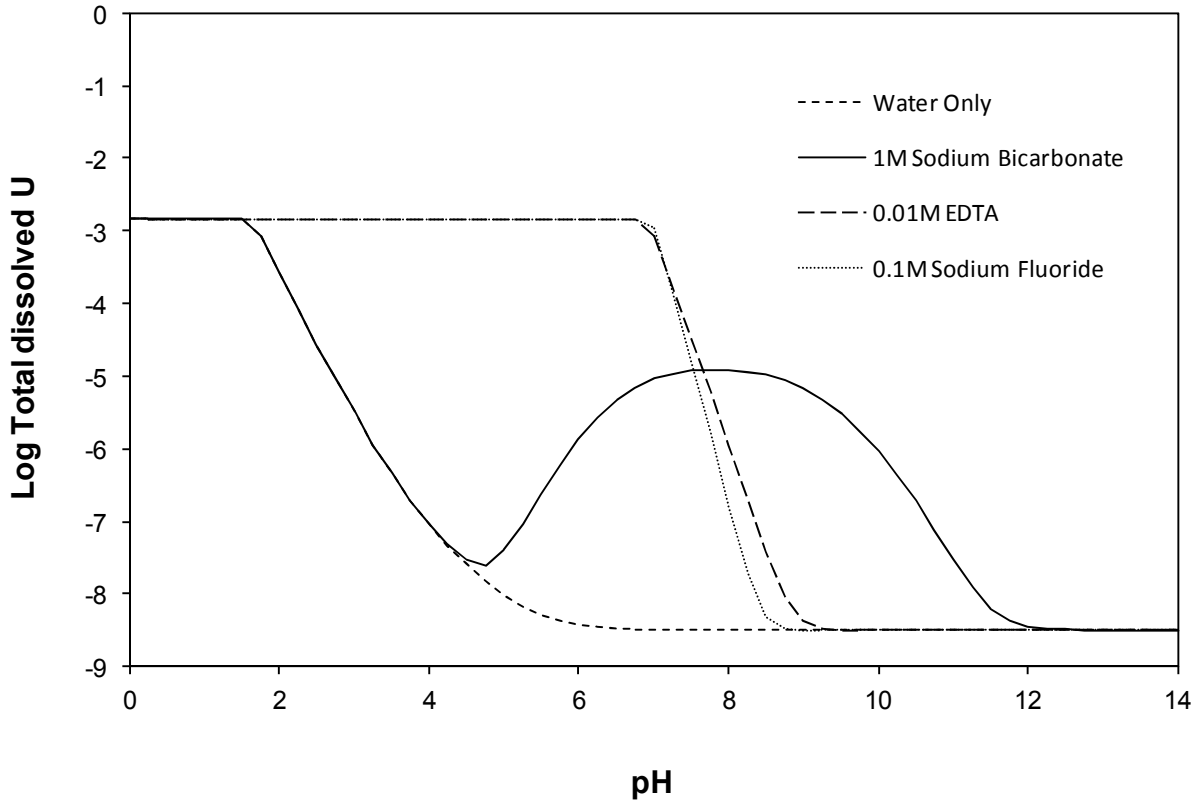

Figure S1. Calculated dissolved uranium for equilibration of 1.48 mM U(IV) (logC = -2.8) with solutions containing different ligands. The calculations were performed in MINEQL+ v. 4.6 with the assumption that all uranium remained in the +IV oxidation state. Concentrations lower than the total amount in the system indicate that U(IV) would be precipitated as uraninite. Both 0.1 M sodium fluoride and 0.01 M sodium EDTA are predicted to completely dissolved 1.48 mM uraninite at pH values less than 7.

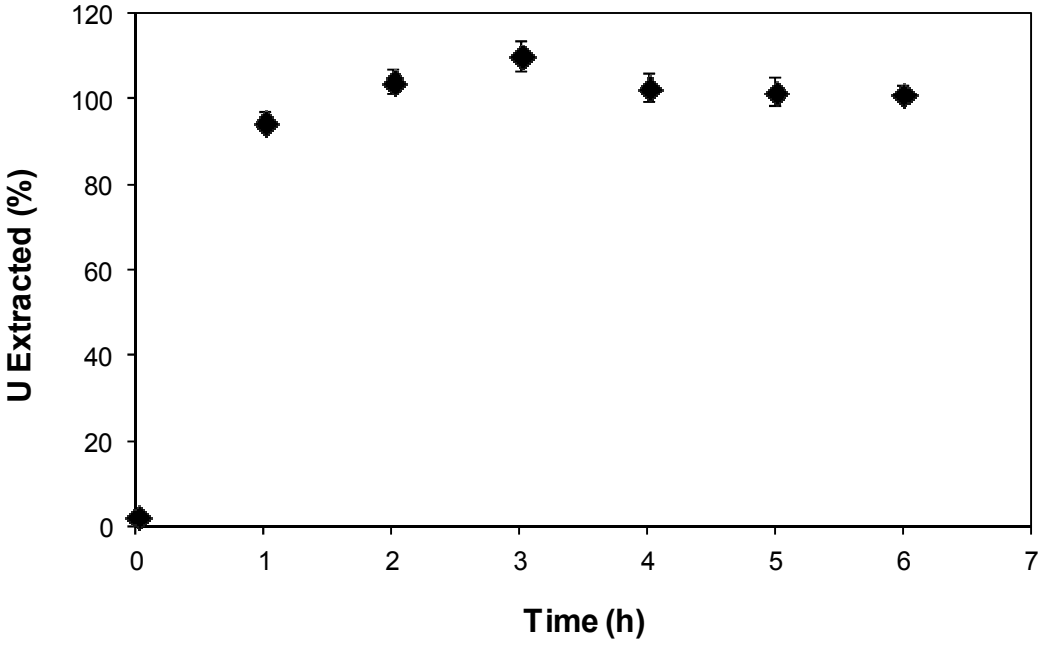

Figure S2. Oxidation experiments on biogenic uraninite not washed with HCO_3^- reacted with 50 mM persulfate and 100 mM HCO3$^-$.

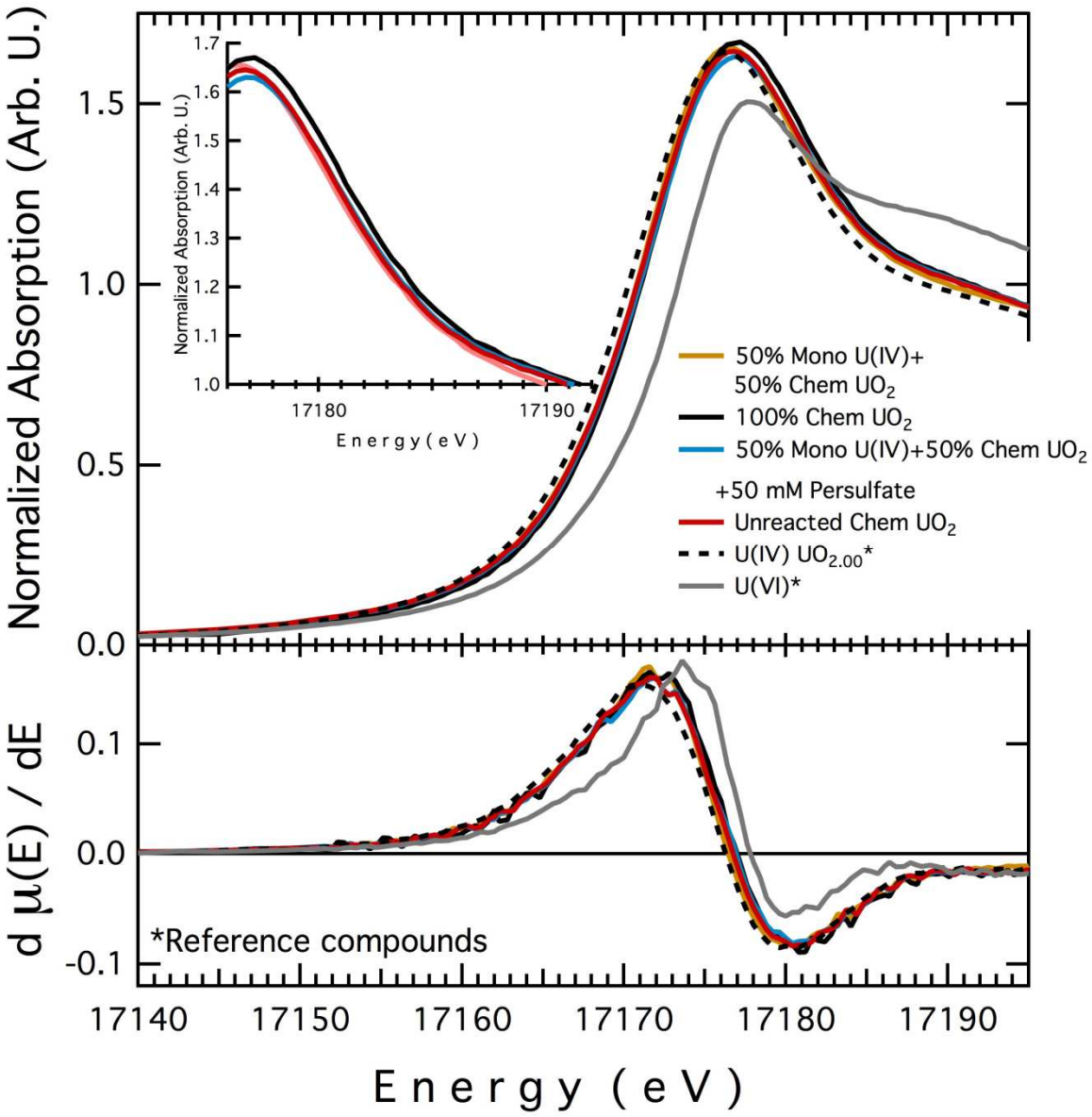

Figure S3. UL_{III}-edge XANES spectra for: 50% chemogenic UO_2 and 50% monomeric U(IV) with 100 mM HCO_3^-); 100% chemogenic UO_2 + 100 mM HCO_3^- + 50 mM $K_2S_2O_8$; 50% chemogenic UO_2 and 50% monomeric U(IV) + 100 mM HCO_3^- + 50 mM $K_2S_2O_8$; un-reacted monomeric U(IV); and monomeric U(IV).

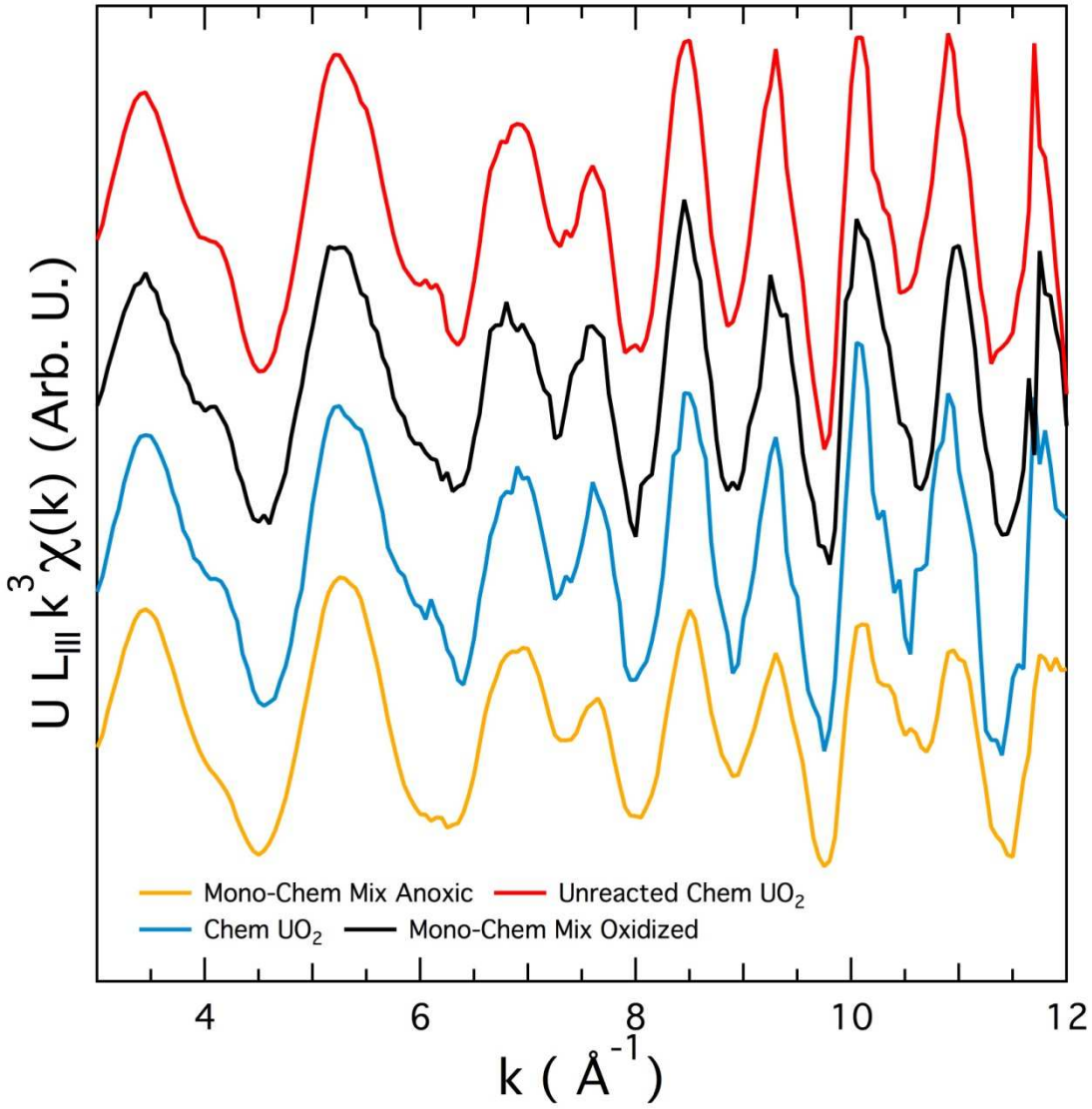

Figure S4. UL$_{III}$-edge EXAFS spectra for 50% chemogenic UO_2 and 50% monomeric U(IV) mixture exposed to 100 mM HCO_3^- both with an oxidant (Mono-Chem Mix Oxidized with 50 mM persulfate) and without (Mono-Chemic Mix Anoxic, control). Chemogenic UO_2 (Chem UO_2) reacted with 50 mM persulfate and an unreacted chemogenic UO_2 material are included for comparison.

Discussion of Optimization of Oxidation Rate Constants

The release of U(VI) to solution following oxidation of various U(IV) species in water containing 8.2 mg L^{-1} dissolved oxygen was interpreted using a first order rate law as described in the manuscript (Eq. 1 in the manuscript and here).

$$\frac{d[U(VI)]}{dt} = k[U(IV)] \quad (1)$$

For the oxidation of the monomeric U(IV) and biogenic uraninite samples, the release of U(VI) was interpreted as the sum the uranium released from each species (Eq. 5 in the manuscript and Eq. 2 here).

$$[U(VI)] = [U(IV)]_{mono,0}\left(1 - e^{-k_{mono}t}\right) + [U(IV)]_{bio-UO_2,0}\left(1 - e^{-k_{bio-UO_2}t}\right) \quad (2)$$

This approach was necessary because based on previous studies neither the monomeric U(VI) nor the biogenic uraninite samples were pure forms of U(VI); the biogenic uraninite included 35% of the U(IV) in monomeric forms, and the monomeric U(IV) sample included 10% of the U(IV) as biogenic uraninite. The rate constants for the two forms of U(IV) included in Eq. 5 were determined by simultaneously optimizing the fit of Eq. 5 to the datasets for both monomeric U(IV) and biogenic uraninite; the initial amounts of monomeric U(IV) and biogenic uraninite for each dataset were set at their known values. In this manner a larger dataset was used to determine the two parameters in Eq. 5. The optimization was performed by a minimizing the sum of squares of the difference between the model output and the experimental data. This least squares of residuals procedure was performed using an optimization routine included in Excel spreadsheet software package. The model simulation for the optimized rate constants is shown together with the experimental data in Figure S5.

For the oxidation of the chemogenic uraninite in the same solution (8.2 mg L^{-1} dissolved oxygen and 100 mM HCO3-), the extent of dissolution was so small that the amount of chemogenic uraninite can be treated as essentially constant over the 6-h experiment duration. Consequently, the rate and rate constant could be determined by linear regression of the dissolved U(VI) concentration versus time (Eq. 3). The concentrations indeed increase linearly, and the data are shown together with the values calculated according to a rate constant of 1.0 x 10^{-9} mol g $U(IV)^{-1}$ s^{-1} (8.9 x 10^{-10} mol g UO_2^{-1} s^{-1}) (Figure S6). The linear increase starts at a concentration greater than zero, which is probably the result of an almost instantaneous release to solution of a trace amount of U(VI) that may have been associated with the chemogenic uraninite.

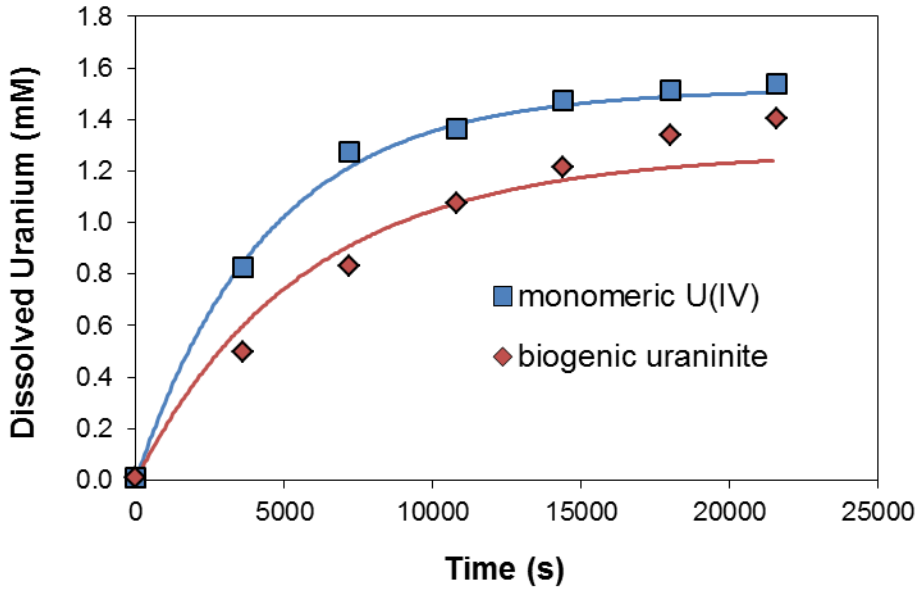

Figure S5. Dissolved U(VI) produced during the oxidation of solid-associated biogenic U(IV) species in a solution with 8.2 mg L^{-1} dissolved oxygen and 100 mM HCO_3^-. The experimental data (points) and the simulation results of a model for first order kinetics (lines) are presented together for comparison.

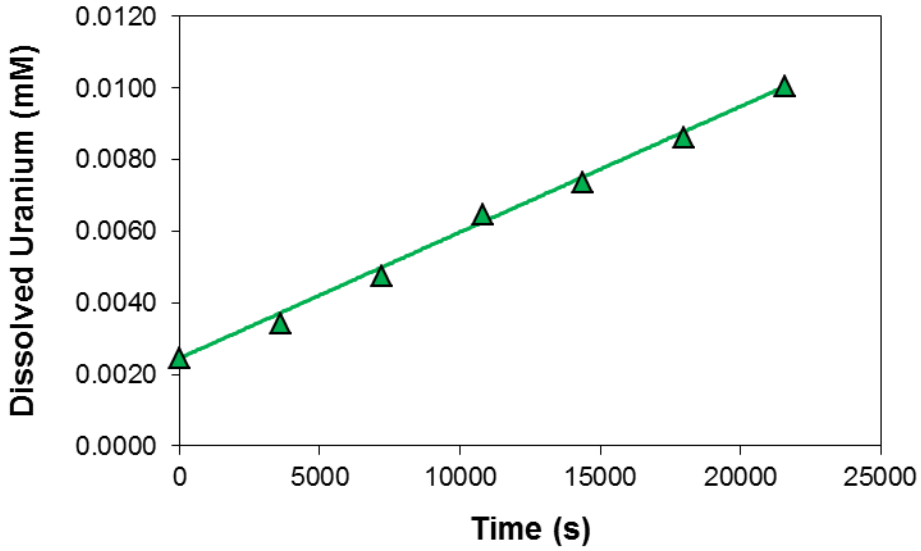

Figure S6. Dissolved U(VI) produced during the oxidation of chemogenic uraninite in a solution with 8.2 mg L^{-1} dissolved oxygen and 100 mM HCO_3^-. The experimental data (points) and the simulation results of a model for first order kinetics (line) are presented together for comparison.